International Journal of Pressure Vessels and Piping 126-127 (2015) 1–7

Contents lists available at ScienceDirect

International Journal of Pressure Vessels and Piping

journal homepage: www.elsevier.com/locate/ijpvp

Strain rate effects on dynamic fracture of pipeline steels: Finite element simulation

P.S. Yu, C.Q. Ru*

Department of Mechanical Engineering, University of Alberta, Edmonton, Alberta T6G 2G8, Canada

ARTICLE INFO

Article history:
Received 2 October 2013
Received in revised form
21 November 2014
Accepted 2 December 2014
Available online 12 December 2014

Keywords:
Finite element
Pipeline steel
Strain rate effect
Cohesive zone model
Speed-dependent
Fracture toughness

ABSTRACT

The present work develops a strain rate-dependent cohesive zone model and related finite element model to analyze speed-dependent dynamic fracture of pipeline steels observed in recent drop-weight tear tests. Different than most of existing cohesive zone models, the traction-separation law of the present model considers the rate of separation in the cohesive zone, and a rate-dependent elastic-viscoplastic constitutive model is employed for the bulk material. The speed-dependences of CTOA and energy dissipation observed experimentally are reproduced in our simulations for moderate steady-state crack speed (up to 150 m/s). The present model gives detailed stress-strain fields surrounding the moving crack tip, which offer plausible explanation why the rate-effects in the bulk material and the cohesive zone could be largely responsible for all observed speed-dependent dynamic fracture phenomena of pipeline steels.

1. Introduction

The weakening effect of increasing crack speed on dynamic fracture toughness of pipeline steel within specific range of crack speed has been revealed in some recent tests [1–4]. However, it is still a challenge to obtain a specific relationship between dynamic fracture toughness and crack speed in a wide range of crack speed due to the expensive costs of experiments. Meanwhile, the dependence of fracture toughness on crack speed and understanding the mechanism of this dependence are critical for material selection and crack-arrest design in high-strength steel pipelines. In the recent work of Ren and Ru [5], a cohesive zone model (CZM) based finite element (FE) model is proposed to simulate the drop-weight tear test (DWTT) of pipeline steel [3]. In their simulations of standard and modified DWTT specimens (the difference between the two kinds of specimens will be shown below) under impact loading, the speed-dependent dynamic fracture toughness of pipeline steel observed in tests [3] and a few related experimental results (including cracking speed, force-displacement curve and CTOA) are reproduced using a simple CZM based on a properly adjusted traction-separation law (TSL). The remarkable agreement between their simulation [5] and the tests [3], within a moderately wide range of cracking speed (roughly from 20 m/s to higher than 100 m/s), suggests that the CZM-based FE model proposed in Ref. [5] could offer a useful method to predict and analyze the speed-dependent dynamic fracture toughness of pipeline steels especially when experimental tests are difficult or too expensive.

However, there are still a few noticeable limitations of the model proposed in Ref. [5] which have to be further explored. In general, dynamic fracture is featured particularly by two key factors: inertia and strain-rate. For pipeline steels, because fracture speed is usually not very high compared to the wave speeds, some researchers believe that the inertia effect could be secondary as compared to strain-rate effect [6]. However, the simulations of Ref. [5] are based on a rate-independent material constitutive model obtained from static uniaxial tension tests. Ignoring strain-rate effect might have led to significant errors in calculating crack-tip stress-strain field, CTOA, crack speed and fracture energy. Actually, in the cohesive zone model used in Ref. [5], the key parameters of TSL (especially their dependence on the crack speed) have been purposely adjusted to fit the known test data [3] without any physical justification based on the tested materials. As a consequence, not surprisingly, some noticeable inconsistencies existed between the simulations [5] and some details of tests of Ref. [3], especially for the high speed cases of modified specimens. For example, the simulations [5] predict that the crack speed is

* Corresponding author. Tel.: +1 780 492 4477; fax: +1 780 492 2200.
E-mail address: cru@ualberta.ca (C.Q. Ru).

http://dx.doi.org/10.1016/j.ijpvp.2014.12.001
0308-0161/

Nomenclature

CTOA	crack tip opening angle, see Fig. 7
CZM	cohesive zone model, see Fig. 2
D	damage scalar in traction-separation law, see Eq. (1)
DWTT	drop-weight tear test
E/A	total energy dissipation per unit cracked face, see Table 2
FE	finite element
G_c	cohesive energy
K	elastic stiffness in traction-separation law, see Eq. (1)
m, n	material constants in rate-dependent constitutive model, see Eq. (3)
MBS$_{0.05}$, **MBS**$_{0.07}$ and **MBS**$_{0.082}$	modified specimen with a back-slot of depth of 0.05 m, 0.07 m and 0.082 m, see Fig. 1
SS	standard specimen, see Fig. 1
T_0, T and T_{max}	rate-independent, rate-dependent and maximum traction stress in cohesive zone, see Eq. (1) and (2), Figs. 3 and 4
TSL	traction-separation law
v	crack speed
α	exponent in traction-separation law, see Eq. (1) and Fig. 3
η, β	coefficient and power exponent in rate-dependent traction-separation law, see Eq. (2) and Fig. 4
$\bar{\varepsilon}^p$, $\bar{\varepsilon}_r$, $\dot{\bar{\varepsilon}}^p$ and $\dot{\bar{\varepsilon}}_r$	equivalent plastic strain, reference strain, equivalent plastic strain-rate and reference strain-rate, see Eq. (3)
$\dot{\bar{\varepsilon}}^p_{max}$	maximum equivalent plastic strain-rate at crack tip, see Table 1
σ_y	static tensile yielding stress
$\bar{\sigma}$	equivalent stress, see Eq. (3)
δ	separation in cohesive zone, see Eq. (1)
δ_0, δ_{max}	separation corresponding to the maximum traction and maximum damage, see Eq. (1)
$\dot{\delta}$, $\bar{\dot{\delta}}$	separation rate and mean separation rate of cohesive element, see Eq. (2) and Table 1

accelerating near the end of fracture process, in contradiction with the tests in which the crack speed is decelerating near the end of fracture process. In addition, the contact force of the hammer predicted by the simulations [5] always decreases with displacement of the hammer much more sharply than the steady-state fracture tests [3].

In the present paper we shall develop a rate-dependent CZM, in which the traction in the cohesive zone depends not only on the separation but also on the rate of separation [7–12] and the surrounding material is governed by a rate-dependent elastic-viscoplastic constitutive model [13–15]. Based on the proposed rate-dependent models, the DWTTs of standard and modified specimens are analyzed using FE simulations. As will be shown below, the present rate-dependent model can reasonably explain speed-dependent dynamic fracture observed in tests [3] and some details of tests which the previous rate-independent model [5] cannot explain. In addition, the strain-stress fields ahead of the crack tip are also analyzed using the present rate-dependent model, which offers a plausible explanation for the speed-dependence of dynamic fracture for pipeline steels. The present rate-dependent model offers an improved numerical method to simulate and analyze some details of dynamic fracture of pipeline steels at high crack speed.

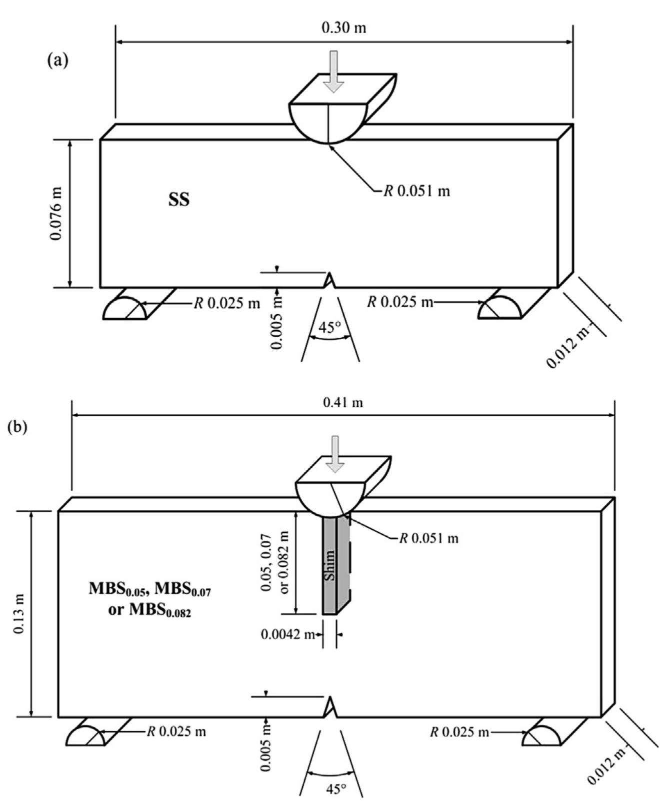

Fig. 1. Geometries of the standard ((a): **SS**) and modified ((b): **MBS**$_{0.05}$, **MBS**$_{0.07}$ and **MBS**$_{0.082}$) specimens of DWTT.

2. The present rate-dependent models

2.1. Geometries of specimens

There are two kinds of specimens tested in the DWTTs [3]. As shown in Fig. 1(a) is a standard DWTT specimen, while (b) is a modified one. Both specimens have an initial static-precracked V-notch with an angle of 45° and a depth of 0.005 m at the middle of bottom. The standard DWTT specimen is a three-dimensional rectangular plate of the dimension of 0.30 m × 0.076 m × 0.012 m, while the modified specimen is a three-dimensional rectangular plate of the dimension of 0.41 m × 0.13 m × 0.012 m with a back-slot cut through the thickness of the specimen. A high-strength shim is inserted into the slot of the modified specimen. There are three different back-slots with a width of 0.042 m and three depths of 0.05 m, 0.07 and 0.082 m. The in-plane size of the modified specimen is larger than the standard one, in order to provide a sufficient ligament for steady-state crack growth. In this paper, the standard specimen will be named as **SS**, while the three modified specimens are named as **MSB**$_{0.05}$, **MBS**$_{0.07}$ and **MBS**$_{0.082}$ based on the depths of the back-slots, respectively. As will be showed below, the modified specimen is designed to achieve faster crack speed. Both specimens are supported by two rigid anvils with a radius of 0.025 m and impacted by a rigid hammer, which has a fixed initial speed of 8 m/s and a variable mass of 100–200 kg [3,16].